Intensive Care Med (2008) 34:361–367
DOI 10.1007/s00134-007-0887-5

EXPERIMENTAL

Satoshi Hagiwara
Hideo Iwasaka
Shigekiyo Matsumoto
Takayuki Noguchi

High dose antithrombin III inhibits HMGB1 and improves endotoxin-induced acute lung injury in rats

Received: 28 November 2006
Accepted: 17 September 2007
Published online: 17 October 2007

Electronic supplementary material
The online version of this article (doi:10.1007/s00134-007-0887-5) contains supplementary material, which is available to authorized users.

This article is discussed in the editorial available at: http://dx.doi.org/10.1007/s00134-007-0888-4.

S. Hagiwara (✉) · H. Iwasaka · S. Matsumoto · T. Noguchi
Oita University Faculty of Medicine, Department of Brain and Nerve Science, Anesthesiology,
1-1 Idaigaoka, Hasamamachi, Yufu City, Oita 879-5593, Japan
e-mail: saku@med.oita-u.ac.jp

Abstract *Objective:* High mobility group box 1 (HMGB1) is an important factor in the development of sepsis. Previous work suggests that antithrombin III (ATIII) inhibits inflammation, but the mechanism of action is still poorly understood. *Design and setting:* Prospective controlled animal study in a university laboratory. *Materials:* Rats were randomly divided into a lipopolysaccharide (LPS)-induced sepsis control group and an ATIII-treated experimental group. Animals in the experimental group received a bolus of 250 units/kg of ATIII injected into the tail vein. *Measurements and results:* Animals receiving high-dose ATIII (250 units/kg) had significantly improved lung histopathology and survival compared to the control rats. We measured serum and lung levels of various cytokines and HMGB1 at regular intervals from 0 to 12 h after the induction of sepsis and demonstrated lower HMGB1 levels over time in ATIII-treated animals. In an in vitro experiment, we stimulated the mouse macrophage cell line RAW 264.7 with LPS in the presence or absence of ATIII. Subsequent measurement of HMGB1 concentrations in the supernatant and cell signaling molecules in cell lysates revealed an ATIII dose-dependent decrease in HMGB1 release. Furthermore, inhibition of IkB and p42 phosphorylation was observed with the administration of ATIII, suggestive of downstream signaling pathways. *Conclusions:* High-dose ATIII decreases lung pathology and reduces mortality in a rat sepsis model. This finding may be mediated by the inhibition of HMGB1.

Keywords Inflammation · Cell signal · Lipopolysaccharide · High mobility group box 1 · Antithrombin III

Introduction

The high fatality rate of sepsis is due to its protean complications throughout major organ systems. Despite recent increases in our understanding of the molecular underpinnings of sepsis, most of these complications remain refractory to treatment [1]. The respiratory system in particular is severely affected and difficult to treat [2].

Initiation of the coagulation cascade and the subsequent production of pro-inflammatory cytokines are central to the pathogenesis of sepsis [3]. The treatment of severe sepsis with anticoagulant agents, which modulate inflammatory reactions in addition to their anticoagulant activity, has been the focus of considerable interest [4, 5]. One such molecule is antithrombin III (ATIII), the primary physiological inhibitor of thrombin and other serine proteases in the clotting cascade. ATIII inhibits cytokine and tissue factor production in endothelial cells and monocytes [6–8]. The clinical potential of ATIII is evidenced by its ability to prevent organ failure and increase survival rates in septic animals [9, 10]. In humans, however, a large-scale clinical trial [11] failed to

demonstrate the efficacy of ATIII among sepsis patients. In contrast, a pre-specified subgroup analysis revealed that patients treated with antithrombin without concomitant heparin administration had more favorable outcomes than those who did not receive antithrombin [12]. Additionally, clinical studies have shown that the administration of ATIII in patients with sepsis reduces organ failure and increases survival in patients with a high risk of death [13, 14]. Such conflicting reports reflect the current lack of understanding of the exact role of ATIII in mediating sepsis.

Recently, High mobility group box 1 (HMGB1) was discovered to play a key role as a late-phase mediator in the pathogenesis of sepsis [15]. HMGB1 is an intranuclear protein originally identified to be important in the regulation of genetic information [16]. During inflammation, HMGB1 mediates cell-to-cell signaling by binding to the receptor for advanced glycosylation end product (RAGE) [17], Toll-like receptor 2 (TLR2) [18, 19], and Toll-like receptor 4 (TLR4) [18, 19]. HMGB1 also acts as a pro-coagulant, thereby enhancing the inflammatory response in septic shock [20]. HMGB1 contributes to the pathology and mortality of sepsis, presumably as an inflammatory mediator [21]. Indeed, HMGB1 is present in the serum of sepsis patients, with higher levels associated with increased mortality [22, 23]. Moreover, specific inhibition of endogenous HMGB1 by anti-HMGB1 antibody reverses the lethality of established sepsis in mice [24].

We hypothesized that ATIII inhibits serum and tissue HMGB1 to prevent acute lung injury in a murine model of sepsis. To test this hypothesis, we investigated the impact of ATIII administration on levels of HMGB1 and lung histopathology in rats with lipopolysaccharide (LPS)-induced sepsis. To further elucidate the mechanism of this effect, we assessed the impact of ATIII on RAW264.7 macrophage cell secretion of HMGB1.

Materials and methods

In vivo study

Materials

ATIII was donated by Mitsubishi Pharma (Osaka, Japan). LPS (O127:B8) was obtained from Sigma (St Louis, MO). All other reagents were of the highest available analytical grade. Antibodies to HMGB1 (Shino-Test, Tokyo, Japan); p50 (Santa Cruz Biotechnology, Santa Cruz, CA); phosphorylated p38, phosphorylated p42, phosphorylated JNK, phosphorylated IKB alpha (p-IkB alpha), IkB alpha (Cell Signaling Technology, Beverly, MA); and beta-actin (Abcam, Cambridge, UK) were purchased.

Animals

Male Wistar rats weighing 250–300 g (Kyudou, Saga, Japan) were used in all experiments. All protocols conformed to the National Institute of Health (NIH) guidelines, and the animals received humane care in compliance with the Principles of Laboratory Animal Care. All animals were housed with access to food and water ad libitum.

Animals were randomly assigned to one of six groups: (1) LPS group ($n = 6$): rats received simultaneous infusion of 0.9% NaCl solution (1.0 ml/kg) and a bolus injection of LPS (7.5 mg/kg) into the tail vein; (2–5) ATIII treatment groups ($n = 6$ per group): rats were infused with different dosages of ATIII (30, 60, 125, 250 units/kg) in separate groups concurrent with a bolus of LPS (7.5 mg/kg) into the tail vein; (6) Negative control group ($n = 6$): rats received infusion of 0.9% NaCl solution (1.0 ml/kg) with a simultaneous bolus of 0.9% NaCl solution (1.0 ml/kg) into the tail vein.

Histological analysis

Lung sections were stained with hematoxylin and eosin. A pathologist blinded to group assignment analyzed the samples and determined levels of lung injury according to Murakami's technique [25]. Briefly, 24 areas in the lung parenchyma were graded on a scale of 0–4 (0, absent, appears normal; 1, light; 2, moderate; 3, strong; 4, intense) for congestion, edema, infiltration of inflammatory cells, and hemorrhaging. Mean scores for each of the parameters were used for analysis.

Measurements of cytokine and HMGB1 secretion

HMGB1, Il-6, and TNF-alpha levels were determined using commercial enzyme-linked immunosorbent assay (ELISA) kits (HMGB1: Shino-Test; IL-6 and TNF-alpha: R&D Systems, Minneapolis, MN). The absorbance at 450 nm was determined using an automated plate reader (Bio-Rad Laboratories, Hercules, CA).

Immunohistochemical analysis

Lung tissue samples were fixed upon resection in 4% paraformaldehyde at 4 °C overnight. Immunohistochemistry was performed after blocking endogenous peroxidase activity. Sections were incubated with anti-HMGB1 polyclonal antibody (1:1000 dilution) and visualized with horseradish peroxidase (HRP) conjugate and diaminobenzidine.

Western blotting

Proteins were resolved by sodium dodecyl sulfate-polyacrylamide gel electrophoresis (SDS-PAGE) and transferred to polyvinylidene difluoride membranes (Millipore, Bedford, MA). Membranes were incubated with primary antibody (1:1000 dilution) for 1 h at room temperature followed by HRP-conjugated secondary antibody (1:1000 dilution, Invitrogen, Carlsbad, CA) for 1 h at room temperature. Blots were subsequently developed using an enhanced chemiluminescence detection kit (Amersham, Buckinghamshire, UK) and exposed on Hyperfilm ECL (Amersham).

In vitro study

The murine macrophage cell line RAW264.7 was maintained in RPMI 1640 media containing 5% heat-inactivated fetal bovine calf serum and antibiotics at 37 °C under 5% CO_2. The media was removed and replaced with RPMI 1640 containing 5% FBS (in most experiments) or Opti-MEM (in experiments designed to measure HMGB1 in conditioned media). RAW264.7 cells were treated with ATIII and simultaneously stimulated with LPS.

NF-kB binding assay

The DNA binding activity of NF-kB (p50/p65) was determined using an ELISA-based nonradioactive NF-kB p50/p65 transcription factor assay kit (Chemicon, Temecula, CA). The absorbance at 450 nm was determined using an automated plate reader (Bio-Rad Laboratories, Hercules, CA).

Statistical analysis

All data were presented as the mean ± standard error of the mean (SEM). Data were analyzed by a one-way analysis of variance (ANOVA) and the unpaired t-test for single comparisons. A p-value of < 0.05 was considered to be statistically significant.

Results

In vivo study

Mortality

LPS administration induced death in 50% of rats that did not receive concurrent ATIII within 12 h. In comparison, at 12 h after LPS administration, 60% of rats that received 30 units/kg of ATIII survived, while 80% of rats that received 60 and 125 units/kg ATIII survived. All rats that received a concurrent high dose of ATIII (250 units/kg) survived up to 7 days after LPS administration, comparable to the saline-treated control animals.

Effect of ATIII on lung tissue

In the negative control group, no pulmonary histological alterations were observed (Fig. 1A–C). Among the LPS-treated rats with sepsis, lung tissue showed edema formation and interstitial infiltration by neutrophils 12 h after LPS administration (Fig. 1D–F). High-dose ATIII (250 units/kg) treatment significantly reduced interstitial edema and inflammatory cell infiltration in comparison to the control group (Fig. 1G–I). Histology scores, based on the number of areas with congestion, edema, inflammation, and hemorrhaging, were significantly higher in the LPS group than in the negative control group. All scores were lower in the ATIII co-administration group than in the LPS-only group.

Effects of ATIII on serum levels of IL-6, TNF-alpha, and HMGB1

Treatment with ATIII (250 units/kg) along with LPS administration significantly decreased IL-6 concentration at all assay times. Similarly, groups treated with ATIII (250 units/kg) showed decreased serum levels of TNF-alpha at all assay times. Serum levels of HMGB1 also increased over time following LPS infusion. This increase was less prominent in rats treated with ATIII

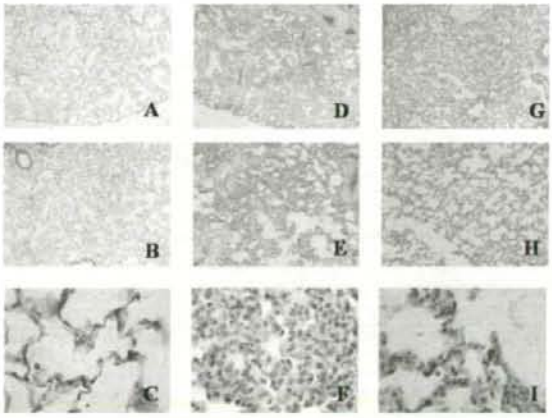

Fig. 1 Effects of ATIII on lung injury in LPS-treated rats. Lung tissue was obtained from rats infused with saline and stained with hematoxylin and eosin (magnifications: **A**, 40×; **B**, 100×; **C**, 400×), LPS (magnifications: **D**, 40×; **E**, 100×; **F**, 400×), or ATIII + LPS (magnifications: **G**, 40×; **H**, 100×; **I**, 400×)

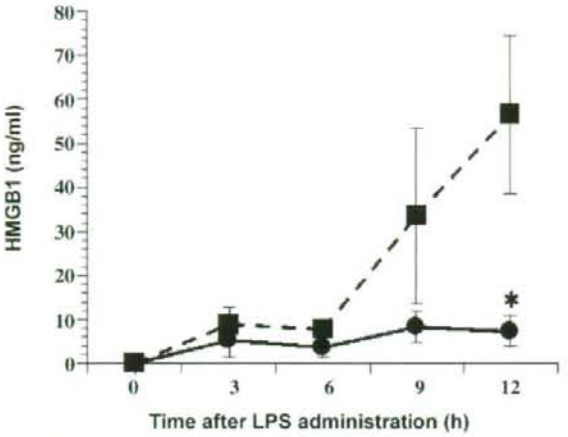

Fig. 2 Temporal changes in serum HMGB1 concentrations after LPS administration in rats. Rats were given either LPS alone (LPS group) or LPS in conjunction with ATIII (ATIII-treated group). HMGB1 serum concentration are shown for both groups ($n = 6$ for each group) at multiple time points after LPS administration. The *dashed line* represents values measured for the LPS group; the *solid line* represents values for the ATIII-treated group. All data are expressed as the mean ± SE. * Significant difference from the LPS group ($p < 0.05$)

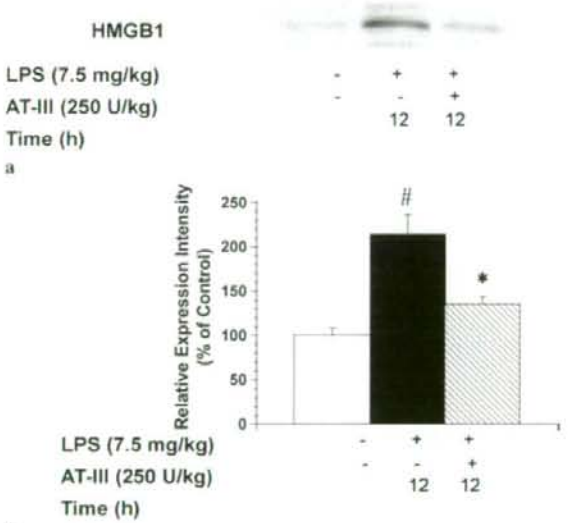

Fig. 3 Changes in HMGB1 protein expression in lung tissue after LPS administration in rats. Rats were given either LPS alone (LPS group) or LPS in conjunction with ATIII (ATIII-treated group); **a** HMGB1 expression in the lung tissue of both groups 12 h after LPS administration was detected by Western blot and quantified by integrated optical densitometry; **b** Expression of HMGB1 protein was normalized to that of the negative control group for each group; # Significant difference from negative control animals ($p < 0.05$); * Significant difference from the LPS group ($p < 0.05$)

(250 units/kg) than in those receiving LPS alone (Fig. 2). Serum levels of IL-6, TNF-alpha and HMGB1 did not increase in the negative control group at any time point assayed (data not shown).

Effect of ATIII on HMGB1 levels in lung tissue

The expression of HMGB1 in lung tissue increased as a result of the LPS infusion. This increase was less pronounced among ATIII (250 unit/kg) treated rats than in the LPS and negative control groups (Fig. 3). Immunohistochemical analyses revealed that cells expressing HMGB1 increased after LPS administration alone. In contrast, the proportion of cells expressing HMGB1 decreased dramatically in the LPS-administered rats treated with ATIII (250 units/kg) (Fig. 3).

In vitro study

Effect of ATIII on secreted and cellular levels of HMGB1

LPS administration increased murine macrophage secretion of HMGB1 levels in culture, which was inhibited by the administration of ATIII. In addition, the inhibition of HMGB1 by ATIII was minimal at a concentration of 1 unit/ml but maximal at 20 units/ml, demonstrating a dose dependence of the ATIII-mediated inhibition (Fig. 4).

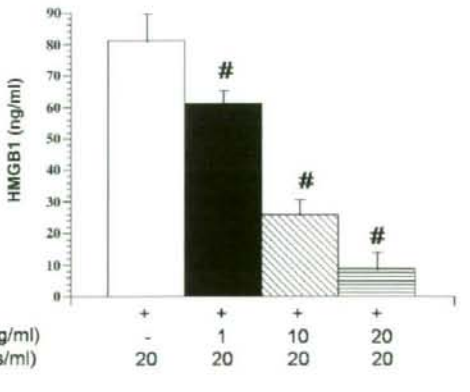

Fig. 4 Effect of ATIII on HMGB1 production by LPS-stimulated murine macrophages. Murine macrophages treated with ATIII were stimulated with LPS for 20 h. Subsequently, conditioned media were collected and HMGB1 levels were determined by ELISA. The *dashed line* represents values measured for the LPS group; the *solid line* represents values for the ATIII-treated group. All data are expressed as the mean ± SE; # Significant difference from the LPS group ($p < 0.05$)

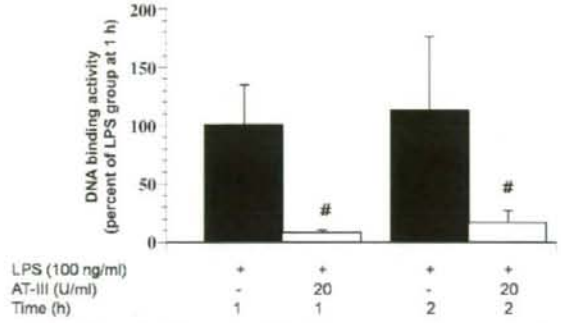

Fig. 5 Effect of ATIII on the LPS-induced increase in the specific binding of p50 and p65 to DNA. Murine macrophages were treated with or without ATIII and stimulated with LPS for 1 or 2 h prior to harvest. The specific binding of p50 or p65 to DNA was analyzed in nuclear extracts by Western blot analysis. Quantification of bands by integrated optical densitometry revealed a marked decrease in the p50/p65 binding activity with AT-III co-administration. All data are expressed as the mean ± SE; # Significant difference from LPS group at 1 h ($p < 0.05$)

Effect of ATIII on secreted cytokines

The TNF-alpha levels in the culture supernatant increased at 1 h after the administration of LPS. In contrast, ATIII administration significantly inhibited the secretion of TNF-alpha. Similarly, LPS administration increased IL-6 levels in the culture supernatant, which was also significantly inhibited by ATIII.

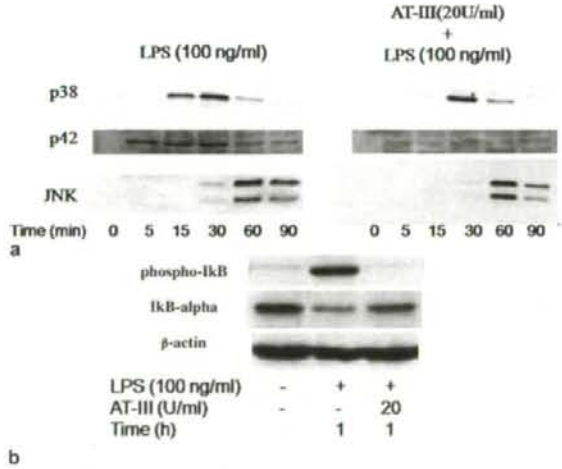

Fig. 6 Effect of ATIII on the LPS-induced phosphorylation of p38, p42, JNK, and IkB. Murine macrophages treated with or without ATIII (20 units/ml) were stimulated with LPS (100 ng/ml) for the indicated time periods. **a** The cytoplasmic levels of phosphorylated p38, p42, and JNK MAPK were determined by Western blot analysis using phospho-specific p38, p42 and JNK MAPK antibodies. **b** The cytoplasmic levels of phosphorylated IkB alpha, IkB alpha, and beta-actin were determined by Western blot analysis using phosphorylated IkB-alpha (phospho-IkB), IkB-alpha, and beta-actin antibodies

ATIII inhibits IKK and MAPK pathways and modulates NF-kB

The p50 and p65 levels in the nucleus of RAW264.7 macrophage cells increased at 1 h after administration of LPS. However, administration of ATIII partially suppressed this increase. Furthermore, treatment of LPS led to a robust activation of the NF-kB transcription factor p50/p65, which was blocked by ATIII (Fig. 5).

The phosphorylation of p32 and JNK in RAW264.7 cells also increased after the administration of LPS, but this was unaffected by ATIII. In contrast, an increase in the phosphorylation of p42 in RAW264.7 cells after LPS administration was reduced by ATIII (Fig. 6).

Treatment with LPS resulted in the degradation of IkB-alpha, which was inhibited by ATIII (Fig. 6). In addition, the phosphorylation of p-IkB-alpha in RAW264.7 cells increased after LPS administration, which was also inhibited by ATIII (Fig. 6b).

Discussion

In a LPS model of sepsis in rats, we demonstrated that treatment with ATIII improved the mortality of rats in endotoxin-induced septic shock in a dose-dependent manner, with a maximum effect at a dose of 250 units/kg. In addition, our findings suggested that infusion of high-dose ATIII at 250 units/kg can prevent acute lung injury. This study also demonstrated increased levels of HMGB1 in serum and lung tissue of an in vivo LPS-induced rat model of sepsis. Furthermore, we revealed that ATIII inhibits secretion of HMGB1 in LPS-stimulated murine macrophages in parallel in vitro experiments.

These results build on the growing body of evidence suggesting the importance of HMGB1 in the initiation of acute lung injury [21] and as a late mediator of lethality in sepsis [26]. Our findings showed that serum levels of cytokine and HMGB1 were not significantly inhibitory at low doses of ATIII. However, the data suggested that ATIII may inhibit not only cytokines in serum, but also HMGB1 in both serum and lung tissue. We surmise that this caused the remarked decrease in mortality among rats treated with high-dose ATIII.

Various pathways have been suspected to underlie the inhibition of HMGB1 secretion. The stimulation of a number of cytokines induces the release of HMGB1 [27]. In the present study, the TNF-alpha and IL-6 levels in the serum were significantly lower in the ATIII-treated group than in the control group. In addition, ATIII inhibited TNF-alpha

and IL-6 in LPS-stimulated murine macrophages in vitro. In particular, previous work supports a potential role for TNF-alpha in the regulation of LPS-induced HMGB1 release [27]. Our results suggest that the inhibition of cytokine secretion by ATIII in sepsis mediates the inhibition of HMGB1.

LPS stimulation of macrophages activates several intracellular signaling pathways, including the IKK-NF-κB pathway and three mitogen-activated protein kinase (MAPK) pathways [28, 29]. We demonstrate that ATIII does not influence the phosphorylation of p38 and JNK in MAPK signaling. On the other hand, ATIII does suppress the activation of NF-kB by preventing the phosphorylation of the main driver of the IKK pathway, IkB, as well as that of p42 of the MAPK pathway. In accordance, the inhibition of the phosphorylation of IkB and p42 after ATIII administration in sepsis may lead to the inhibition of NF-kB activation.

When NF-kB is phosphorylated after the stimulation of cells by LPS, NF-kB coordinates the induction of many genes encoding the production and secretion of pro-inflammatory cytokines [30]. In addition, the activation of NF-kB contributes to the secretion of HMGB1 after LPS administration [31]. We demonstrated that ATIII inhibits LPS-induced NF-kB activation, and this may in turn inhibit the secretion of HMGB1. Nevertheless, the mechanism by which ATIII decreases HMGB1 secretion and expression remains unknown.

In conclusion, our results suggest that high-dose ATIII might therapeutically benefit septic patients not only due to its anticoagulant activity, but also due to its ability to inhibit the production and secretion of HMGB1. ATIII may inhibit the inflammatory response in sepsis while improving lung injury and survival rate. As a caveat, this study only examined the short-term therapeutic effects of ATIII at 12 h after onset of lethal endotoxemia. In addition, we have no evidence as to the effect of delayed administration of ATIII or the HMGB1 mRNA expression in LPS-induced septic shock models, which require further study.

Acknowledgements. The authors wish to thank Dr. Tomohisa Uchida for giving helpful advice and for scoring lung injuries.

References

1. Andrews P, Azoulay E, Antonelli M, Brochard L, Brun-Buisson C, Dobb G, Fagon JY, Gerlach H, Groeneveld J, Mancebo J, Metnitz P, Nava S, Pugin J, Pinsky M, Radermacher P, Richard C, Tasker R (2006) Year in review in intensive care medicine, 2005. II. Infection and sepsis, ventilator-associated pneumonia, ethics, haematology and haemostasis, ICU organisation and scoring, brain injury. Intensive Care Med 32:380–390
2. Andrews P, Azoulay E, Antonelli M, Brochard L, Brun-Buisson C, Dobb G, Fagon JY, Gerlach H, Groeneveld J, Mancebo J, Metnitz P, Nava S, Pugin J, Pinsky M, Radermacher P, Richard C, Tasker R, Vallet B (2005) Year in review in intensive care medicine, 2004. I. Respiratory failure, infection, and sepsis. Intensive Care Med 31:28–40
3. Iba T, Kidokoro A, Yagi Y (1998) The role of the endothelium in changes in procoagulant activity. J Am Coll Surg 87:321–329
4. Freeman BD, Zehnbauer BA, Buchman TG (2003) A meta-analysis of controlled trials of anticoagulant therapies in patients with sepsis. Shock 20:5–9
5. Matthay MA (2001) Severe sepsis: a new treatment with both anticoagulant and anti-inflammatory properties. N Engl J Med 344:759–762
6. Uchiba M, Okajima K (1997) Antithrombin III (AT III) prevents LPS-induced pulmonary vascular injury: novel biological activity of AT III. Semin Thromb Hemost 23:583–590
7. Totzke G, Schobersberger W, Schloesser M, Czechowski M, Hoffmann G (2001) Effects of antithrombin III on tumor necrosis factor-alpha and interleukin-1beta synthesis in vascular smooth muscle cells. J Interferon Cytokine Res 21:1063–1069
8. Inthorn D, Hoffmann JN, Hartl WH, Muhlbayer D, Jochum M (1998) Effect of antithrombin III supplementation on inflammatory response in patients with severe sepsis. Shock 10:90–96
9. Yang S, Hauptman JG (1994) The efficacy of heparin and antithrombin III in fluid-resuscitated cecal ligation and puncture. Shock 2:433–437
10. Iba T, Kidokoro A, Fukunaga M, Nagakari K, Suda M, Yoshikawa S, Ida Y (2005) Antithrombin ameliorates endotoxin-induced organ dysfunction more efficiently when combined with danaparoid sodium than with unfractionated heparin. Intensive Care Med 8:1101–1108
11. Warren BL, Eid A, Singer P, Pillay SS, Carl P, Novak I, Chalupa P, Atherstone A, Penzes I, Kubler A, Knaub S, Keinecke HO, Heinrichs H, Schindel F, Juers M, Bone RC, Opal SM, KyberSept Trial Study Group (2001) High-dose antithrombin III in severe sepsis. A randomized controlled trial. J Am Med Assoc 286:1869–1878
12. Iba T, Kidokoro A (2004) What can we learn from the three mega-trials using anticoagulants in severe sepsis? Shock 22:508–512
13. Wiedermann CJ, Hoffmann JN, Juers M, Ostermann H, Kienast J, Briegel J, Strauss R, Keinecke HO, Warren BL, Opal SM, KyberSept Investigators (2006) High-dose antithrombin III in the treatment of severe sepsis in patients with a high risk of death: efficacy and safety. Crit Care Med. 34:285–292
14. Mammen EF (1998) Antithrombin III and sepsis. Intensive Care Med 7:649–650
15. Wang H, Bloom O, Zhang M, Vishnubhakat JM, Ombrellino M, Che J, Frazier A, Yang H, Ivanova S, Borovikova L, Manogue KR, Faist E, Abraham E, Andersson J, Andersson U, Molina PE, Abumrad NN, Sama A, Tracey KJ (1999) HMG-1 as a late mediator of endotoxin lethality in mice. Science 285:248–251
16. Bustin M (1999) Regulation of DNA-dependent activities by the functional motifs of the high-mobility-group chromosomal proteins. Mol Cell Biol 19:5237–5246
17. Fiuza C, Bustin M, Talwar S, Tropea M, Gerstenberger E, Shelhamer JH, Suffredini AF (2003) Inflammation-promoting activity of HMGB1 on human micro vascular endothelial cells. Blood 101:2652–2660

18. Yu M, Wang H, Ding A, Golenbock DT, Latz E, Czura CJ, Fenton MJ, Tracey KJ, Yang H (2006) HMGB1 signals through toll-like receptor (TLR) 4 and TLR2. Shock 26:174–179
19. Park JS, Gamboni-Robertson F, He Q, Svetkauskaite D, Kim JY, Strassheim D, Sohn JW, Yamada S, Maruyama I, Banerjee A, Ishizaka A, Abraham E (2006) High Mobility Group Box 1 protein (HMGB1) interacts with multiple Toll like receptors. Am J Physiol Cell Physiol 290:917–924
20. Sunden-Cullberg J, Norrby-Teglund A, Treutiger CJ (2006) The role of high mobility group box-1 protein in severe sepsis. Curr Opin Infect Dis 19:231–236
21. Ueno H, Matsuda T, Hashimoto S, Amaya F, Kitamura Y, Tanaka M, Kobayashi A, Maruyama I, Yamada S, Hasegawa N, Soejima J, Koh H, Ishizaka A (2004) Contributions of high mobility group box protein in experimental and clinical acute lung injury. Am J Respir Crit Care Med 170:1310–1316
22. Hatada T, Wada H, Nobori T, Okabayashi K, Maruyama K, Abe Y, Uemoto S, Yamada S, Maruyama I (2005) Plasma concentrations and importance of High Mobility Group Box protein in the prognosis of organ failure in patients with disseminated intravascular coagulation. Thromb Haemost 94:975–979
23. Sunden-Cullberg J, Norrby-Teglund A, Rouhiainen A, Rauvala H, Herman G, Tracey KJ, Lee ML, Andersson J, Tokics L, Treutiger CJ (2005) Persistent elevation of high mobility group box-1 protein (HMGB1) in patients with severe sepsis and septic shock. Crit Care Med 33:564–573
24. Yang H, Ochani M, Li J, Qiang X, Tanovic M, Harris HE, Susarla SM, Ulloa L, Wang H, DiRaimo R, Czura CJ, Wang H, Roth J, Warren HS, Fink MP, Fenton MJ, Andersson U, Tracey KJ (2004) Reversing established sepsis with antagonists of endogenous high-mobility group box 1. Proc Natl Acad Sci USA 101:296–301
25. Murakami K, McGuire R, Cox RA, Jodoin JM, Bjertnaes LJ, Katahira J, Traber LD, Schmalstieg FC, Hawkins HK, Herndon DN, Traber DL (2002) Heparin nebulization attenuates acute lung injury in sepsis following smoke inhalation in sheep. Shock 18:236–241
26. Yang H, Wang H, Tracey KJ (2001) HMG-1 rediscovered as a cytokine. Shock 15:247–253
27. Wang H, Vishnubhakat JM, Bloom O, Zhang M, Ombrellino M, Sama A, Tracey KJ (1999) Proinflammatory cytokines (tumor necrosis factor and interleukin 1) stimulate release of high mobility group protein-1 by pituicytes. Surgery 126:389–392
28. Kwak HJ, Song JS, Heo JY, Yang SD, Nam JY, Cheon HG (2005) Roflumilast inhibits lipopolysaccharide-induced inflammatory mediators via suppression of nuclear factor-kappaB, p38 mitogen-activated protein kinase, and c-Jun NH2-terminal kinase activation. J Pharmacol Exp Ther 315:1188–1195
29. Schottelius AJ, Mayo MW, Sartor RB, Baldwin AS (1999) Interleukin-10 signaling blocks inhibitor of kappaB kinase activity and nuclear factor kappaB DNA binding. J Biol Chem 274:1868–1874
30. Adcock IM (1997) Transcription factors as activators of gene transcription: AP-1 and NF-kappa B. Monaldi Arch Chest Dis 52:178–186
31. Dumitriu IE, Baruah P, Valentinis B, Voll RE, Herrmann M, Nawroth PP, Arnold B, Bianchi ME, Manfredi AA, Rovere-Querini P (2005) Release of high mobility group box 1 by dendritic cells controls T cell activation via the receptor for advanced glycation end products. J Immunol 174:7506–7515

Journal of Surgical Research **145,** 251–256 (2008)
doi:10.1016/j.jss.2007.06.012

Effect of Enteral *Versus* Parenteral Nutrition on LPS-Induced Sepsis in a Rat Model

Satoshi Hagiwara, M.D., Ph.D.,[1] Hideo Iwasaka, M.D., Ph.D., Shigekiyo Matsumoto, M.D., and Takayuki Noguchi, M.D., Ph.D.

Department of Brain and Nerve Science, Anesthesiology, Oita University Faculty of Medicine, Oita, Japan

Submitted December 25, 2006

Background. **The purpose of the present study was to determine whether total enteral nutrition (TEN) or total parenteral nutrition (TPN) differ in their modulation of ghrelin production and cardiac dysfunction induced by lipopolysaccharide (LPS).**

Materials and methods. **Vascular catheters or gastrostomy tubes were surgically placed into rats who received isocaloric parenteral or enteral nutrition postoperatively. After 7 d, the rats were injected intravenously with LPS (2.5 mg/kg). Serum ghrelin levels were determined by enzyme-linked immunosorbent assay and myocardiac function was assessed via the Langendorff isolated heart technique.**

Results. **Before and after the administration of LPS, TEN was found to be more effective at increasing the plasma ghrelin levels than TPN. After LPS administration, left-ventricular developed pressure decreased in animals receiving TPN when compared with animals receiving TEN. Animals receiving TPN also had significant reductions in their maximal rates of increase ($+dp/dt_{max}$) and decrease ($-dp/dt_{max}$) in left ventricular pressure when compared with animals receiving TEN (unpaired *t*-test, $P < 0.05$). Upon reperfusion after 30 min of ischemia, the left ventricular resting tension decreased in animals receiving TPN compared with animals receiving TEN. Thereafter, left-ventricular developed pressure, $+dp/dt_{max}$, and $-dp/dt_{max}$ decreased in the TEN recipients in comparison to the TPN-receiving animals.**

Conclusions. **We conclude that TEN more effectively increases plasma ghrelin levels than TPN. The maintenance of higher ghrelin levels in TEN-fed rats is associated with maintaining cardiac function during LPS-induced septic shock.**

Key Words: **ghrelin; parenteral nutrition; enteral nutrition; sepsis; ischemic-reperfusion.**

INTRODUCTION

Ghrelin is a newly discovered hormone produced principally in the stomach, which has been identified as the endogenous ligand for the growth hormone secretagogue receptor [1]. The hormone is a physiological mediator of feeding, and is believed to play a role in growth regulation by stimulating feeding and the release of growth hormones [2]. Ghrelin also plays other roles in humans, including providing beneficial effects in patients suffering from septic shock [3]. In particular, ghrelin and its receptors have been detected in cardiovascular tissues, and are believed to have a protective effect against ischemic damage to the heart [4, 5].

No information is available concerning whether the route of nutritional support (parenteral *versus* enteral) affects the components of the ghrelin system. The route of nutritional support in catabolic patients and experimental animals modulates a number of critical aspects in host defense, including bacterial translocation, immune function, hormone secretion, and cytokine production [6]. Because ghrelin is known to increase food intake and is secreted predominantly from the stomach [7, 8], different routes of nutritional support may modulate ghrelin synthesis and secretion.

In this study, we investigated whether total enteral nutrition (TEN) and total parenteral nutrition (TPN) differed in their effects on serum ghrelin levels and cardiac ischemia caused by lipopolysaccharide (LPS)-induced sepsis shock.

[1] To whom correspondence and reprint requests should be addressed at Department of Brain and Nerve Science, Anesthesiology, Oita University Faculty of Medicine, 1-1 Idaigaoka-Hasamamachi, Yufu City, Oita 879-5593, Japan. E-mail: saku@med.oita-u.ac.jp.

0022-4804/08 $34.00

MATERIALS AND METHODS

Animals and Surgical Procedures

Male Wistar rats weighing 250 to 300 g (Kyudou, Saga, Japan) were housed at a constant temperature, exposed to a 12:12-h light-dark cycle and water ad libitum, for 1 wk before experiments were initiated. Prior to surgery, cefotiam hydrochloride was administered to each rat. Animals were anesthetized using sevoflurane (3%) and oxygen. All surgeries were performed using sterile technique. Rats in the control group (n = 15) were allowed free access to non-purified rat diet and water. A sham midline laparotomy was performed on the animals in this group. Rats in the TEN group (n = 15) received a midline laparotomy during which a catheter was inserted into the anterior wall of the stomach, followed by suturing to the stomach wall, and exteriorization through the antero-lateral abdominal wall. The catheter was then subcutaneously tunneled to the shoulder region. Catheters were exteriorized between the scapulae, passed through a tightly coiled stainless steel spring, and connected through a freely rotating swivel (Instech, Plymouth Meeting, PA) to a 50 mL syringe pump (Nipro). For the animals in the TPN group (n = 15), a small-gauge silicone catheter was inserted into the right internal jugular vein (within 0.5 cm of the heart) using aseptic technique, and secured with 4.0 silk sutures. The free end of the catheter was tunneled subcutaneously and exteriorized between the shoulders through a stainless steel reinforced silicone anchoring plate (Instech). The catheter was then passed through a flexible stainless steel protective spring and attached via a freely rotating swivel (Instech) to a 50 mL syringe pump (Nipro). A sham midline laparotomy was performed on the animals in this group as well. After surgery, the animals were housed in wire-bottom cages and fasted overnight, but had free access to water.

All procedures involving rats were conducted according to the guidelines for the care and use of laboratory animals approved by our institution.

Nutritional Support

The morning following the surgical procedure, a continuous infusion of either TEN or TPN was started and maintained for the subsequent 7 d. Nutritional support was prepared and infused under sterile conditions. TEN formulation contained (all amounts per liter) 21.9 g of amino acids, 11.15 g of lipids, and 78.1 g of carbohydrates in addition to various vitamins and minerals (Racol; Otsuka, Tokyo, Japan). Animals received approximately 60 kcal · kg^{-1} · day (0.5 kcal/mL × 2 mL/h). The parenteral formulation was composed of TPN solution (Hicaliq NC-H; Terumo, Tokyo, Japan) containing essential and nonessential amino acids (Amiparen 10%; Otsuka, Tokyo, Japan), yielding a mixture that was isocaloric compared with the enteral preparation. TPN formulation contained (all amounts per liter) 28.56 g of amino acids and 178.5 g of carbohydrates in addition to various minerals. Animals received approximately 60 kcal/kg^{-1}/d (0.5 kcal/mL × 2 mL/h). After receiving either enteral or parenteral nutrition for 7 d, TPN and TEN were stopped and animals were given an i.v. injection of LPS (2.5 mg/kg) (O127:B8; Sigma, St. Louis, MO). Blood samples (0.3 mL) were obtained under sevoflurane anesthesia at 0, 3, 6, and 12 h after LPS administration to determine plasma ghrelin levels.

Histological Analysis

Stomachs were extracted from animals 12 h after LPS (2.5 mg/kg) administration under the administration of sevofluren anesthesia. Stomach tissue specimens were instilled with 10% formalin. The samples were embedded in paraffin, and cut into 4-μm sections. Sections were stained with hematoxylin and eosin.

Mucosal Thickness

Gastric mucosal thickness was measured using an image analysis system (Axio Vision AC Ver. 4.4; Carl Zeiss Vision GmbH, Standort Göttingen, Vertrieb, Germany), and a Zeiss microscope (Oberkochen, Germany), at a magnification of ×400. For each sample, at least 15 fields were used. Mean values, expressed in microns, were obtained, and results were grouped according to the treatment.

Measurements of Ghrelin Secretions

Ghrelin concentrations in plasma were determined using commercial rat enzyme-linked immunosorbent assay (ELISA) kits (Phoenix Pharmaceuticals, Inc., Burlingame, CA). Serum samples were assayed using the ELISA sandwich method. Ninety-six well plates were precoated with monoclonal antibodies specific to rat ghrelin. The samples, negative controls, and diluted ghrelin standard markers were added to each well. The detection of ghrelin in the samples was performed according to the manufacturer's protocol. A450 values were subsequently determined using an ELISA reader.

Immunohistochemical Analysis

Immunohistochemistry was performed after blocking the endogenous peroxidase activity from rat's stomach tissue with 1% H2O2 and 10% sheep serum. Blocked sections of stomach tissue were incubated with anti-ghrelin monoclonal antibody (1:1000 dilution) overnight at 4°C. The sections were then incubated with peroxidase-conjugated anti-mouse IgG. The slides were stained using the LSAB2 kit (DACO Via Real, Carpinteria, CA) as the biotin avidin peroxidase complex system. After development, the slides were counterstained with Mayer's hematoxylin and mounted.

Immunoblotting Analysis

The hearts were harvested from animals following 7 d of respective nutrition treatments. After the blood was washed out using saline perfusion, the heart was homogenized with a T-PER tissue protein extraction reagent (PIERCE, Rockford, IL) in a polytron homogenator (IKA Labortechnik, Staufen, Germany). The homogenates were then centrifuged at 10,000 × g for 5 min at 4°C. The concentration of protein in the collected supernatant was measured by absorbance at 562 nm using the BCA protein assay regent system (Pierce, Rockford, IL).

For gel electrophoresis, equal quantities of protein (100 μg) were suspended in sodium dodecyl sulfate-polyacrylamide gel electrophoresis (SDS-PAGE) buffer. Protein samples were boiled for 1 min and separated using a 10% sodium dodecyl sulfate-polyacrylamide gel. Protein runs using SDS-PAGE were immediately electrotransferred to polyvinylidene difluoride membrane (Millipore, Bedford, MA) at 60 V for 3 h in a wet transfer system containing 20 mM Tris-HCl/0.2M glycine in 20% methanol as the transfer buffer. The membrane was blocked with 5% nonfat dry milk in Tris/Tween buffer (25 mM Tris-HCl and 2% Tween 20 (Bio-Rad Lab., Hercules, CA) in 0.14 M NaCl solution) overnight at 4°C.

Polyclonal anti-ghrelin antibody was purchased from Trans Genic Inc. (Kumamoto, Japan). The immune serum was diluted 500-fold with 1% nonfat dry milk and incubated with gentle shaking for 1 h. The polyvinylidene difluoride membrane was then rinsed three times with TBS/Tween buffer for 10 min. The secondary antibody was diluted 1000-fold with 1% nonfat dry milk and incubated with the membrane for 1 h. The blot was then washed by rinsing with TBS/Tween three times for 10 min. The membrane was treated with enhanced chemiluminescence reagent (Amersham, Buckinghamshire, England) and then exposed to X-ray film. After scanning the X-ray film, the band concentration was calculated by quantification of the integrated absorbance using NIH Image J software package (National Institute of Health, Bethesda, MD).

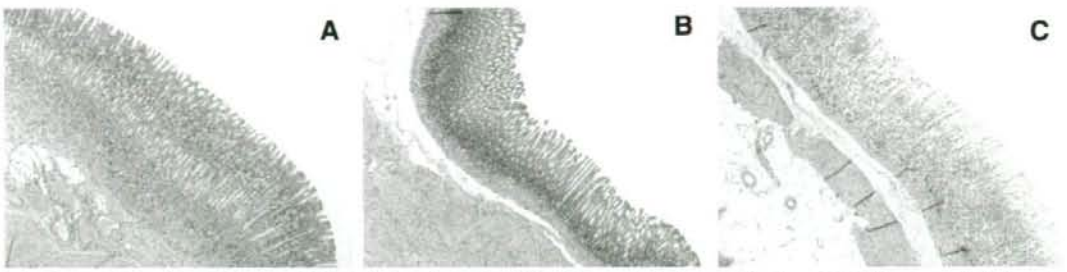

FIG. 1. Stomach histology 12 h after LPS administration, H and E staining, original magnification ×100. The stomach of the animals in the control group exhibited minimal histological damage (A). Animals in the TEN group showed few histological alterations (B). Massive mucosal atrophy was seen in the animals in the TPN group (C). (Color version of figure is available online.)

Isolated Heart Perfusion and the Assessment of the Cardiac Function

Cardiac function was determined by a modified isovolumetric Langendorff technique as described elsewhere [9–11]. Cardiac function is represented in terms of the left ventricular developed pressure (LVDP), left ventricular end-diastolic pressure (LVEDP), and the maximal rates of increase ($+dp/dt_{max}$) and decrease ($-dp/dt_{max}$). Upon termination of the experiments, the beating hearts were rapidly excised into oxygenated Krebs-Henseleit solution containing (in mmol/L) 11 glucose, 2.0 $CaCl_2$, 4.3 KCl, 25 $NaHCO_3$, 118 NaCl, 1.2 $MgSO_4$, and 1.2 KH_2PO_4. Normothermic retrograde perfusion was performed with the same solution in an isovolumetric and nonrecirculating mode. The perfusion buffer was saturated with a gas mixture of 95% O_2-5% CO_2, and pH of 7.4. Perfusion pressure was maintained at 75 mmHg. A latex balloon was inserted through the left atrium into the left ventricle, and the balloon was filled with water (0.18–0.28 mL). LVDP, LVEDP, $+dp/dt_{max}$, and $-dp/dt_{max}$ were continuously recorded using a computerized pressure amplifier-digitizer. A three-way stopcock was mounted above the aortic cannula to create global ischemia. After 20 min of perfusion (equilibration), the hearts were subjected to 30 min of normothermic global ischemia followed by 30 min of reperfusion. The ischemic hearts were placed in a perfusate-filled organ bath chamber. Myocardial temperature was maintained at 37°C by circulating warm water.

Statistical Analysis

All data are presented as mean ± standard error of the mean (SEM). Data were analyzed with analysis of variance and Scheffe's post-hoc test for group pairs for multiple comparisons, as well as by the unpaired *t*-test for single comparisons. A *P*-value less then 0.05 was considered to be statistically significant.

RESULTS

The Effects of TEN or TPN on Stomach Tissue Specimens

We investigated whether TEN or TPN in the rat might change the histological properties of stomach tissue. While the stomach mucosa demonstrated atrophy and the mucosal thickness in the gastric was significantly decreased ($P < 0.05$) in the TPN group compared with the control group (Fig. 1C and Table 1), no histological alterations were observed in either the control or the TEN groups (Fig. 1A and B).

Effects of TPN or TEN on the Serum Levels of ghrelin

Before the LPS administration in the rat, the serum levels of ghrelin were significantly higher in the TEN groups than in the TPN group. After the LPS administration in the rat, the serum levels of ghrelin significantly increased in the TEN group. The peak value was observed 6 h after LPS administration. However, the serum levels of ghrelin were not observed to change in the TPN group. In addition, in the TPN group, the ghrelin concentrations were lower at all assay times (Fig. 2).

The Effects of TPN or TEN on Ghrelin in Stomach Tissue Specimens

According to our immunohistochemical analysis, cells expressing ghrelin were readily observed in the TEN-treated group (Fig. 3A). In contrast, the percentage of ghrelin cells decreased dramatically in the TPN-treated group (Fig. 3B).

The Effects of TPN or TEN on Ghrelin Concentrations in Heart Tissue Specimens

Our immunoblotting analysis revealed that ghrelin protein was readily observed in the heart tissues of TEN-treated and control group animals. In contrast, ghrelin protein was decreased dramatically in the TPN-treated group (Fig. 4).

TABLE 1

Thickness of the Gastric Mucosa

	Mucosa
Control	492.983 ± 34.616
TPN	502.303 ± 16.181
TEN	420.093 ± 26.369*

Note. Values, in μm, are means ± SE.
* $P < 0.05$ relative to mucosal thickness in the control group.

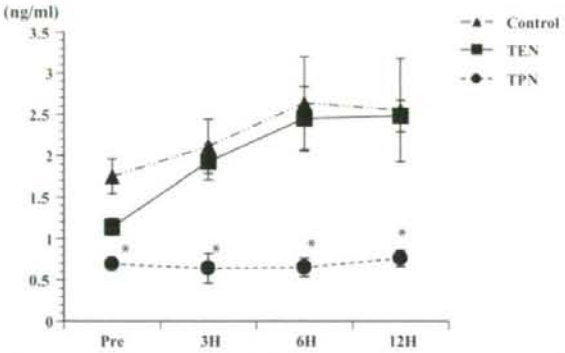

FIG. 2. Effects of LPS administration on the serum levels of ghrelin. All animals were given 2.5 mg/kg LPS i.v. ghrelin serum concentrations at indicated times are shown for each of the groups. Filled triangles represent the control group, filled circles represent the TPN group, and the filled squares represent the TEN-treated group. All data are expressed as the means ± SE. Statistically significant *($P < 0.05$) with respect to the control group animals.

Myocardial Function

There was a significant decrease in LVDP, $+dp/dt_{max}$ and $-dp/dt_{max}$ in the TPN-treated group animals compared with the TEN-treated and control groups. However, no significant changes in LVEDP were observed in any of the groups before I/R. Following I/R there was a significant ($P < 0.05$) decrease in LVDP in each of the groups (Fig. 5A). The recovery of LVDP in the postischemic period was significantly better in the TEN-treated group than in the TPN-treated and control group animals. The LVEDP increased in response to I/R, as shown in Fig. 5B. TEN-treated group animals demonstrated a lower LVEDP at each time point after ischemia, compared with the TPN-treated and control groups ($P < 0.05$). Both $+dP/dt$ and $-dP/dt$ were impaired after ischemia (Fig. 5C, D). However, during reperfusion, both $+dP/dt$ and $-dP/dt$ decreased in the TPN-treated group in comparison to the TEN-treated and control group animals.

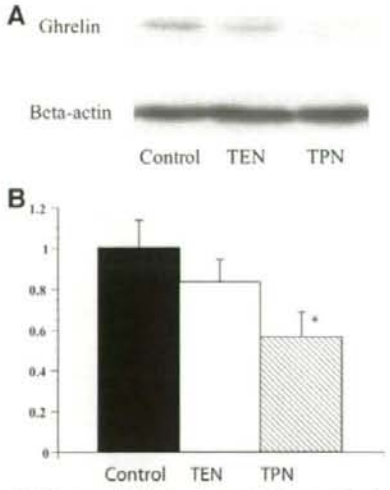

FIG. 4. (A) Immunoblot showing ghrelin protein in the heart tissue of control, TEN, and TPN group animals. (B) Signal intensities for the density of ghrelin protein immunoblot bands. Ghrelin protein levels were quantified using an image analyzer. Expression intensities of ghrelin are shown as the percentages of the control. Data are expressed as the means ± SE. *$P < 0.05$ relative to the control group.

DISCUSSION

In the present study, we demonstrated that total enteral nutrition (TEN) was more effective than total parental nutrition (TPN) at maintaining cardiac function in a rat model of LPS-induced septic shock. Enteral nutrition is currently the preferred method of feeding critically ill patients unless obvious contraindications such as ileus or active gastrointestinal bleeding are present. In addition, a recent study on the use of TEN *versus* TPN for early initiation of enteral nutrition revealed that early use of enteral nutrition was associated with reduced infectious morbidity in critically ill patients [6, 13, 14]. Perioperative or postop-

FIG. 3. Immunohistochemical staining for the presence of ghrelin in the stomach. (A) Rats that underwent sham operations were used as controls. After 7 d, animals received an i.v. injection of LPS (2.5 mg/kg); 12 h following the administration of LPS, the stomachs were harvested from the animals; original magnification ×400. (B) TEN group animals received a continuous infusion of TEN formulation for 7 d. After 7 d, rats received an i.v. injection of LPS (2.5 mg/kg); 12 h following the administration of LPS, the stomachs were harvested from the animals; original magnification ×400. (C) TPN group animals received a continuous infusion of TPN formulation for 7 d. After 7 d, rats received an intravenous injection of LPS (2.5 mg/kg); 12 h following the administration of LPS, the stomachs were harvested from the animals; original magnification ×400. (Color version of figure is available online.)

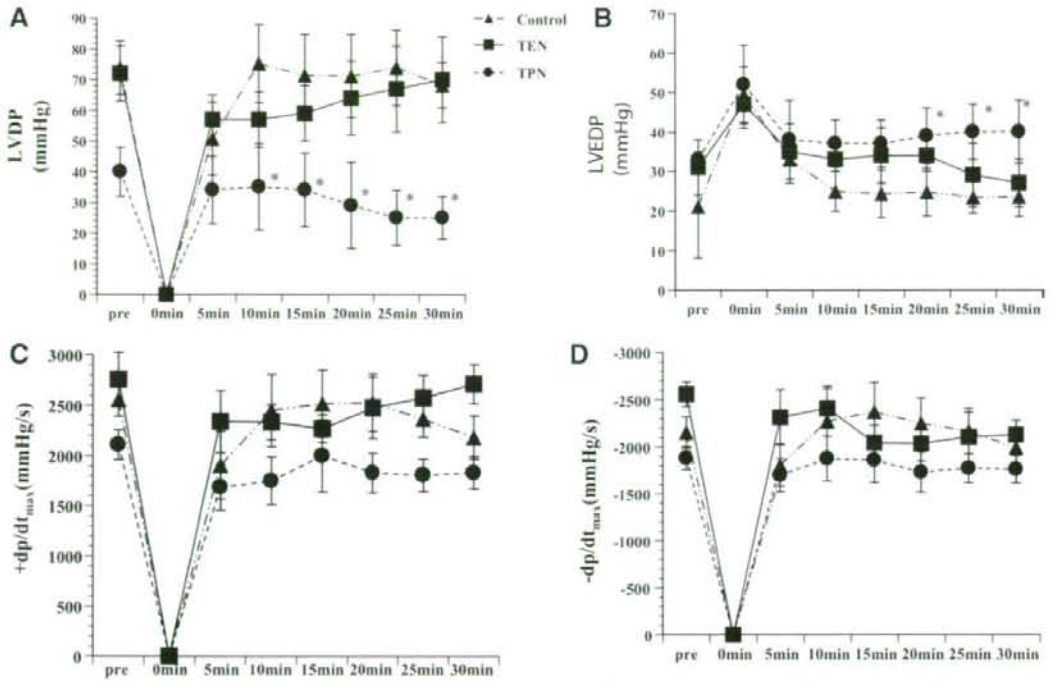

FIG. 5. Changes in the myocardial function after ischemia and reperfusion in the control group, TEN group, and TPN group rat hearts perfused with modified Krebs-Henseleit solution. (A) Left ventricular (LV) developed pressure; (B) LV end-diastolic pressure; (C) the positive value of the first derivative of pressure (+dP/d*t*); (D) the negative value of the first derivative of pressure (−dP/d*t*). Results are expressed as means ± SE. $^*P < 0.05$ relative to control group ischemia-reperfusion (I/R) at corresponding time points in (A)–(D).

erative enteral feeding has been shown to decrease morbidity in both postsurgical and trauma patients in comparison to TPN [12–14]. These findings suggest that TEN is more useful than TPN for providing nutritional support to patients with a variety of conditions.

Whether this conclusion also applies to septic patients is an important issue to resolve, given that such patients experience muscle wasting, immune dysfunction, and declining visceral protein status [15]. Early and adequate nutritional support has therefore been identified as a crucial component in the treatment of a septic patient [16]. In this study, we showed that TEN protected cardiac function in septic shock better than TPN.

Ghrelin may be an important mediator of this observation. Ghrelin has been reported at high levels in rats with endotoxic shock. It has been observed that endotoxin induces the production and release of ghrelin from gastric mucosal cells, and the administration of ghrelin decreases mortality while improving metabolic and hemodynamic disturbances in rats with endotoxic shock [3, 17]. Including type 1a growth hormone secretagogue receptor (GHSR-1a) expression is up-regulated and vascular sensitivity to ghrelin stimulation increases in the hyperdynamic phase of sepsis. The cardiovascular responsiveness to ghrelin has been shown to increase in the hyperdynamic phase of sepsis [18]. In addition, treatment with ghrelin may help correct hemodynamic and metabolic abnormalities in rats experiencing septic shock [19]. In this study, we observed that the expression of ghrelin was significantly increased by the administration of LPS in rats treated with TEN. On the other hand, we did not find any up-regulation of ghrelin in the TPN-treated group. In concordance with these observations, the cardiac function was found to be better in the TEN-treated group when compared with the TPN-treated group at 12 h after LPS administration.

Increasing evidence supports a functional role of ghrelin in myocardial growth, which is associated with improved cardiac function. Ghrelin has been detected in the aorta and myocardium, thus indicating that ghrelin may modulate the cardiovascular parameters through growth hormone-independent mechanisms [20]. In addition, ghrelin protects against myocardial I/R injury during reperfusion [4]. In the TEN-treated group, the expression of ghrelin increased in comparison to the TPN-treated group, thereby protecting cardiac function during sepsis.

This superiority of TEN to TPN was also observed when we evaluated the effect of the nutrition delivery system on gastric mucosa. Mucosal atrophy is due to a combination of decreases in functional stimulation and the absence of normal hormonal, biliary, and pancreatic secretion [21]. On the other hand, enteral nutrition protects the gut from mucosal atrophy. TEN improves gut oxygenation and prevents gut atrophy [22]. In addition, animal studies have shown that the administration of TPN results in significant intestinal villus atrophy within a few days [23]. In this study, we found atrophy of the gastric mucosa in the TPN-treated group. Ghrelin-expressing cells were in lower numbers in the TPN-treated group when compared with the TEN-treated group.

In summary, TEN was found to better maintain serum ghrelin levels and cardiac function following LPS administration in rats. These results suggest that enteral nutrition may reduce the occurrence of organ dysfunction during septic shock when compared with parenteral nutrition. As a caveat, this study examined TEN *versus* TPN effects on cardiac function in rats after endotoxemia. In addition, given that there is no evidence of the effects of ghrelin in TPN-treated rats, further research is needed on the effects of ghrelin *versus* no ghrelin administration in TPN-treated rats.

ACKNOWLEDGMENTS

The authors thank Dr. Tomohisa Uchida for giving helpful advice and for conducting histological and immunohistochemical analysis.

REFERENCES

1. Kojima M, Hosoda H, Date Y, et al. Ghrelin is a growth-hormone-releasing acylated peptide from stomach. Nature 1999;402:656.
2. Nakazato M, Murakami N, Date Y, et al. A role for ghrelin in the central regulation of feeding. Nature 2001;409:194.
3. Chang L, Zhao J, Yang J, et al. Therapeutic effects of ghrelin on endotoxic shock in rats. Eur J Pharmacol 2003;473:171.
4. Chang L, Ren Y, Liu X, et al. Protective effects of ghrelin on ischemia/reperfusion injury in the isolated rat heart. J Cardiovasc Pharmacol 2004;43:165.
5. Gnanapavan S, Kola B, Bustin SA, et al. The tissue distribution of the mRNA of ghrelin and subtypes of its receptor. GHS-R in humans. J Clin Endocrinol Metab 2002;87:2988.
6. Minard G, Kudsk KA. Nutritional support and infection: Does the route matter? World J Surg 1998;22:213.
7. Tschop M, Smiley DL, Heiman ML. Ghrelin induces adiposity in rodents. Nature 2000;407:908.
8. Wren AM, Seal LJ, Cohen MA, et al. Ghrelin enhances appetite and increases food intake in humans. J Clin Endocrinol 2001; 86:5992.
9. Meng X, Ao L, Brown JM, et al. Nitric oxide synthase is not involved in cardiac contractile dysfunction in a rat model of endotoxemia without shock. Shock 1997;7:111.
10. Meng X, Brown JM, Ao L, et al. Norepinephrine induces cardiac heat shock protein 70 and delayed cardioprotection in the rat through 1 adrenoceptors. Cardiovasc Res 1996;32:374.
11. Meng X, Brown JM, Ao L, et al. Endotoxin induces cardiac HSP70 and resistance to endotoxemic myocardial depression in rats. Am J Physiol 1996;271:C1316.
12. Marik PE, Zaloga GP. Early enteral nutrition in acutely ill patients: A systematic review. Crit Care Med 2001;29:2264.
13. Kudsk KA. Early enteral nutrition in surgical patients. Nutrition 1998;14:541.
14. McClave SA, Snider HL, Spain DA. Preoperative issues in clinical nutrition. Chest 1999;115:64.
15. Griffiths RD. Nutrition support in critically ill septic patients. Curr Opin Clin Nutr Metab Care 2003;6:203.
16. Perez J, Dellinger RP. International Sepsis Forum. Other supportive therapies in sepsis. Intensive Care Med 2001;27:116.
17. Korbonits M, Goldstone AP, Gueorguiev M, et al. Ghrelin—a hormone with multiple functions. Front Neuroendocrinol 2004; 25:27.
18. Wu R, Zhou M, Cui X, et al. Up-regulation of cardiovascular ghrelin receptor occurs in the hyperdynamic phase of sepsis. Am J Physiol Heart Circ Physiol 2004;287: 1296.
19. Chang L, Du JB, Gao LR, et al. Effect of ghrelin on septic shock in rats. Acta Pharmacol Sin 2003;24:45.
20. Katugampola S, Davenport A. Emerging roles for orphan G-protein-coupled receptors in the cardiovascular system. Trends Pharmacol Sci 2003;24:30.
21. Weser E, Bell D, Tawil T. Effects of octapeptide-cholecystokinin, secretin, and glucagon on intestinal mucosal growth in parenterally nourished rats. Dig Dis Sci 1981;26: 409.
22. Alpers DH. Enteral feeding and gut atrophy. Curr Opin Clin Nutr Metab Care 2002;5:679.
23. Miura S, Tanaka S, Yoshioka M, et al. Changes in intestinal absorption of nutrients and brush border glycoproteins after total parenteral nutrition in rats. Gut 1992;33:484.

ELSEVIER

Cardiovascular Pathology 17 (2008) 129–138

CARDIOVASCULAR PATHOLOGY

Original Article

C-reactive protein induces high-mobility group box-1 protein release through activation of p38MAPK in macrophage RAW264.7 cells

Ko-ichi Kawahara[a], Kamal Krishna Biswas[a], Masako Unoshima[b], Takashi Ito[a], Kiyoshi Kikuchi[a], Yoko Morimoto[a], Masahiro Iwata[c], Salunya Tancharoen[d], Yoko Oyama[a], Kazunori Takenouchi[a], Yuko Nawa[a], Noboru Arimura[a], Meng Xiao Jie[a], Binita Shrestha[a], Naoki Miura[a], Toshiaki Shimizu[a], Kentaro Mera[c], Shin-ichiro Arimura[a], Noboru Taniguchi[a], Hideo Iwasaka[b], Sonshin Takao[e], Teruto Hashiguchi[a], Ikuro Maruyama[a,*]

[a]*Department of Laboratory and Vascular Medicine Cardiovascular and Respiratory Disorders Advanced Therapeutics, Kagoshima University Graduate School of Medical and Dental Science, Kagoshima 890-8520, Japan*
[b]*Department of Anesthesiology, Oita University Faculty of Medicine, Oita 879-5593, Japan*
[c]*Department of Dermatology, Kagoshima University Graduate School of Medical and Dental Science, Kagoshima 890-8520, Japan*
[d]*Department of Pharmacology, Faculty of Dentistry, Mahidol University, Bangkok 10400, Thailand*
[e]*Frontier Science Research Centre, Kagoshima University, Kagoshima 890-8520, Japan*

Received 30 September 2006; received in revised form 7 August 2007; accepted 22 August 2007

Abstract

Background: C-reactive protein (CRP) is widely used as a sensitive biomarker for inflammation. Increasing evidence suggests that CRP plays a role in inflammation. High-mobility group box-1 (HMGB1), a primarily nuclear protein, is passively released into the extracellular milieu by necrotic or damaged cells and is actively secreted by monocytes/macrophages. Extracellular HMGB1 as a potent inflammatory mediator has stimulated immense curiosity in the field of inflammation research. However, the molecular dialogue implicated between CRP and HMGB1 in delayed inflammatory processes remains to be explored. **Methods and results:** The levels of HMGB1 in culture supernatants were determined by Western blot analysis and enzyme-linked immunosorbent assay in macrophage RAW264.7 cells. Purified CRP induced the release of HMGB1 in a dose- and time-dependent fashion. Immunofluorescence analysis revealed nuclear translocation of HMGB1 in response to CRP. The binding of CRP to the Fcγ receptor in RAW264.7 cells was confirmed by fluorescence-activated cell sorter analysis. Pretreatment of cells with IgG–Fc fragment, but not IgG–Fab fragment, efficiently blocked this binding. CRP triggered the activation of p38MAPK and ERK1/2, but not Jun N-terminal kinase. Moreover, both p38MAPK inhibitor SB203580 and small interfering RNA significantly suppressed the release of HMGB1, but not the MEK1/2 inhibitor U-0126. **Conclusion:** We demonstrated for the first time that CRP, a prominent risk marker for inflammation including atherosclerosis, could induce the active release of HMGB1 by RAW264.7 cells through Fcγ receptor/p38MAPK signaling pathways, thus implying that CRP plays a crucial role in the induction, amplification, and prolongation of inflammatory processes, including atherosclerotic lesions.

Keywords: HMGB1; CRP; Atherosclerosis; Fcγ receptor; p38MAPK

1. Introduction

C-reactive protein (CRP), so named for its capacity to precipitate the somatic C-polysaccharide of *Streptococcus pneumoniae*, has been described as a nonspecific acute-phase reactant protein and a sensitive marker of inflammation and

This study was supported by research grants from the Ministry of Education, Culture, Sports, Science, and Technology of Japan; Grants-in-Aid 17100007 (to S. Takao) and 18791341 (to T. Ito); and Health and Labor Sciences Research Grant from the Ministry of Health, Labor, and Welfare (to I. Maruyama).

* Corresponding author. Tel.: +81 99 275 5437; fax: +81 99 275 2629.
E-mail address: rinken@m3.kufm.kagoshima-u.ac.jp (I. Maruyama).

1054-8807/08/$ – see front matter © 2008 Elsevier Inc. All rights reserved.
doi:10.1016/j.carpath.2007.08.006

tissue damage. Recently, an increased level of CRP has been described in the serum of patients suffering from cardiovascular events [1]. Recent studies have shown that the CRP protein is expressed in macrophages and vascular smooth muscle cells (VSMCs) in atheromatous plaques [2–5] and plays a role in the progression and vulnerability of atherosclerotic lesions [6–12]. Thus, therapeutic inhibition of CRP can represent a new approach to cardiovascular diseases [13]. However, little is known about whether and how CRP acts as a progressive and prolongation factor in cardiovascular disease.

We have recently shown that CRP is colocalized with high-mobility group box-1 (HMGB1) in atherosclerotic lesions [14]. The nuclear protein HMGB1 is present in many eukaryotic cells and has been identified as a late-phase mediator in septic shock [15,16]. HMGB1 consists of two tandem domains designated as HMG boxes A and B, and a highly acidic carboxyl-terminus. HMGB1 appears to have two distinct functions in cellular systems. First, it acts as an intracellular regulator of the transcription process and plays a crucial role in maintenance of DNA functions [17]. Second, HMGB1 is released into the extracellular space by all eukaryotic cells upon necrosis or by macrophages in response to inflammatory stimuli such as lipopolysaccharide (LPS), tumor necrosis factor-α (TNF-α), interleukin (IL) 1, and interferon-γ (IFN-γ) through mitogen-activated protein kinase (MAPK) signal transduction pathways and can act as a potent proinflammatory cytokine through a multiligand receptor for advanced glycation endproducts (RAGE) [18,19]. Through RAGE, HMGB1 stimulates macrophages to release cytokines such as TNF-α, IL-6, and IL-1β [19], suggesting that extracellular HMGB1 plays a critical role in several inflammatory diseases such as septic shock, lung inflammation, and rheumatoid arthritis [15,19,20]. Recently, it has been reported that macrophages are the major cell type responsible for HMGB1 production in human atherosclerotic lesions and that HMGB1 plays a role in the pathogenesis of plaque formation and progression [21]. Accumulating evidence indicates that CRP induces the expression of macrophage chemoattractant protein-1 (MCP-1), IL-6, IL-8, intercellular adhesion molecule-1 (ICAM-1), and vascular cell adhesion molecule-1 (VCAM-1) [10,22,23]; however, to the best of our knowledge there have been no reports demonstrating a linkage between CRP (an acute-phase reactant) and HMGB1 (a late-phase mediator of inflammation).

The present study was undertaken to investigate the effect of CRP on the secretion of HMGB1 using a murine macrophage cell line, RAW264.7, and the underlying intracellular signal transduction pathways involved.

2. Materials and methods

2.1. Antibodies

Anti-HMGB1 antibody was obtained from SHINO-TEST (Kanagawa, Japan). Anti-phospho (p)-ERK1/2, anti-p-p38MAPK, anti-p-Jun N-terminal kinase (JNK), and anti-β-actin antibodies were purchased from Cell Signaling Technology (Beverly, MA).

2.2. MAPK inhibitors and p38MAPK small interfering RNA

Specific inhibitors of p38MAPK (SB203580; Calbiochem, La Jolla, CA) or MAPK kinase (MEK1/2) (U-0126; Promega, Madison, WI), and small interfering RNA (siRNA) for mouse p38MAPK (Santa Cruz Biotechnology, Inc., Santa Cruz, CA) were used to evaluate the functional role of MAPKs in CRP-induced HMGB1 release.

2.3. Purification of CRP

CRP (human) was purchased from Wako Chemicals (Kyoto, Japan). CRP was purified (to remove possible biologic contaminants such as sodium azide and LPS) as described previously [14]. In brief, CRP was filtered with Amicon-Ultra 4 (10,000 molecular weight cut off; Millipore Corporation, Bedford, MA) at 4°C and then washed twice with 20 ml of 0.9% NaCl solution in an intravenous solution (Otsuka, Tokushima, Japan). After CRP had been washed, its concentrations were measured using a commercial enzyme-linked immunosorbent assay (ELISA) kit specific for human CRP (Alpha Diagnostic International, Texas). The contents of LPS in purified CRP solutions (5, 10, 20, 40, and 80 μg/ml) were found to be <5 pg/ml, as determined by Limulus endotoxin assays. The purity of CRP preparations was determined by 12.5% sodium dodecyl sulfate–polyacrylamide gel electrophoresis (SDS-PAGE). A 25-kDa single band corresponding to CRP was obtained by staining gels with sensitive silver staining and by Western blot analysis indicating the purity of CRP. In some experiments, the purified CRP was immunoprecipitated with anti-CRP antibody (Dako Cytomation, Denmark) or nonimmune control IgG (Dako Cytomation), followed by a 16-h incubation of protein G agarose (Santa Cruz Biotechnology, Inc.). The immunoprecipitated proteins were separated by centrifugation, and supernatants were collected for cell stimulation. Experiments were performed with the purified CRP, unless stated otherwise.

2.4. Cell culture

Murine macrophage-like RAW264.7 cells were obtained from the American Type Culture Collection (Manassas, VA) and maintained in RPMI 1640 medium (Gibco BRL, Grand Island, NY) supplemented with 10% fetal bovine serum and 2 mM glutamine.

2.5. Stimulation of macrophage RAW264.7 cells with CRP, mouse IgG, Fc, and Fab fragments

Before stimulation with human-purified CRP, heat-inactivated CRP, a supernatant obtained by immunoprecipitation

(IP) of the purified CRP with anti-CRP antibody or nonimmune control IgG, mouse IgG–Fc fragment (1 μM), mouse IgG–Fab fragment (1 μM), and RAW264.7 cells (2×10^6 cells/6-cm dish) were starved for 2 h with serum-free Opti-MEM-I medium and then stimulated with the aforesaid stimulants in the presence of serum-free Opti-MEM-I medium. Following treatment, HMGB1 levels in culture media were analyzed by Western blot analysis and ELISA.

2.6. Flow cytometry analysis

To block the Fcγ receptor, RAW264.7 cells [5×10^5 cells/tube (100 μl)] were incubated with or without mouse IgG–Fc fragment (Jackson ImmunoResearch Laboratories, Inc., West Grove PA) and mouse IgG–Fab fragment (Jackson ImmunoResearch Laboratories, Inc.) for 30 min at room temperature (RT). Then cells were incubated with CRP (20 μg/ml) for 30 min at RT. Cells were fixed with OptiLyse C (250 μl; Immunotech, Marseille, France) for 15 min and then washed with phosphate-buffered saline (PBS). Washed cells were incubated with anti-CRP antibody (Dako Cytomation) diluted 1:100 with PBS for 60 min. After the cells had been washed, they were incubated with fluorescein isothiocyanate (FITC)-labeled anti-rabbit IgG (Immunotech) diluted 1:50 with PBS for 30 min. Data were analyzed by flow cytometry (Beckman Coulter).

2.7. Preparation of HMGB1 samples for Western blot analysis

Preparations of HMGB1 samples were undertaken as described previously [14]. Following CRP treatment, the culture supernatant (2 ml) was incubated with 50 μl of heparin–Sepharose 6B (heparin beads) for 4 h and then washed thrice with 10 mM phosphate buffer (pH 7.0). Next, 50 μl of sample buffer [62.5 mM Tris–HCl (pH 6.8), 2% SDS, 10% glycerol, and 0.002% bromophenol blue] was added to the washed heparin beads and boiled for 5 min.

2.8. Western blot analysis

Western blot analyses were performed as described previously [19]. Briefly, cell lysates (50 μg) obtained from CRP-treated RAW264.7 cells or HMGB1 samples (40 μl) extracted from heparin beads were subjected to 12% SDS-PAGE, then separated proteins were transferred onto a nitrocellulose membrane (Amersham Biosciences, Piscataway, NJ). The membrane was blocked with 5% nonfat dry milk in Tris-buffered saline (pH 7.4) containing 0.02% Tween 20 (TBST) for 1 h at RT, then incubated with anti-HMGB1 antibody (2 μg/ml) in TBST containing 1% nonfat dry milk for 3 h at RT. After the membrane had been washed, it was incubated with horseradish-peroxidase-conjugated anti-rabbit IgG polyclonal antibody (Santa Cruz Biotechnology, Inc.) diluted 1:3000 in TBST containing 2.5% nonfat dry milk for 1 h at RT. The membrane was washed for a second time, then immunoreactive bands were visualized using an ECL detection system (Amersham Biosciences).

2.9. ELISA analysis

The levels of HMGB1 and TNF-α in cultured supernatants were determined using a commercial ELISA kit specific for human HMGB1 (SHINO-TEST) and TNF-α (R&D Systems, Minnesota), respectively. All experiments were performed in triplicate.

2.10. Annexin V analysis

RAW264.7 cells (2×10^6 cells/6-cm dish) were cultured for 24 h. Cells were then washed with Opti-MEM-I medium (Gibco BRL) and stimulated with or without CRP (20 μg/ml) for 24 h. The cells were incubated with FITC-labeled Annexin V (MBL, Nagoya, Japan) for 5 min. Data were analyzed by flow cytometry (Beckman Coulter).

2.11. Immunofluorescence analysis

To investigate the translocation of HMGB1, RAW264.7 cells were cultured on Lab-Tek chamber slides (Nalge Nunc International, Cambridge, MA) and incubated with CRP (20 μg/ml) for 16 h. Following stimulation, cells were fixed with 2% paraformaldehyde containing 0.2% Triton X-100 (Sigma-Aldrich, St. Louis, MO) for 15 min. Slides were then blocked in 1% bovine serum albumin in PBS containing 0.1% Triton X-100 (PBST) for 1 h and incubated with rabbit anti-HMGB1 polyclonal antibody (1 μg/ml) or normal rabbit IgG as a control for 30 min at RT. Slides were then washed with PBST and incubated with FITC-conjugated anti-rabbit IgG (Immunotech) diluted 1:50 in PBST for 20 min at RT. Finally, cell nuclei were labeled with 4′,6-diamidino-2-phenylindole (DAPI; Nakalai Tesque, Kyoto, Japan). Slides were then washed and examined using an Axioskop microscope (Carl Zeiss, Oberkochen, Germany).

2.12. MTT assay

Cell viability was analyzed by mitochondrial respiratory activity measured using MTT [3-(4,5-dimethylthiazol-2yl)-2,5-diphenol tetrazolium bromide] assay (Wako Chemicals), as described previously [24]. Briefly, cells were cultured in 96-well plates (with 100 μl/well medium) in the absence or in the presence of CRP (20 μg/ml) for 16 h. Then cells were incubated with MTT (20 μl of 2.5 μg/ml per well) for 3 h. Formazan product was solubilized by the addition of 100 μl of dimethyl sulfoxide for 16 h. Dehydrogenase activity was expressed as absorbance at a test wavelength of 570 nm and at a reference wavelength of 630 nm.

2.13. p38MAPK siRNA transfection analysis

RAW264.7 cells (8×10^5 cells/ml) cultured in 6-cm dishes for 24 h were washed with Opti-MEM-I medium (Gibco BRL) and then transfected with siRNA (20 μM) or control siRNA (Santa Cruz Biotechnology, Inc.) using oligofectamine (Gibco BRL) for 2 days. Transfected cells were treated with CRP (20 μg/ml) for 20 h, and culture

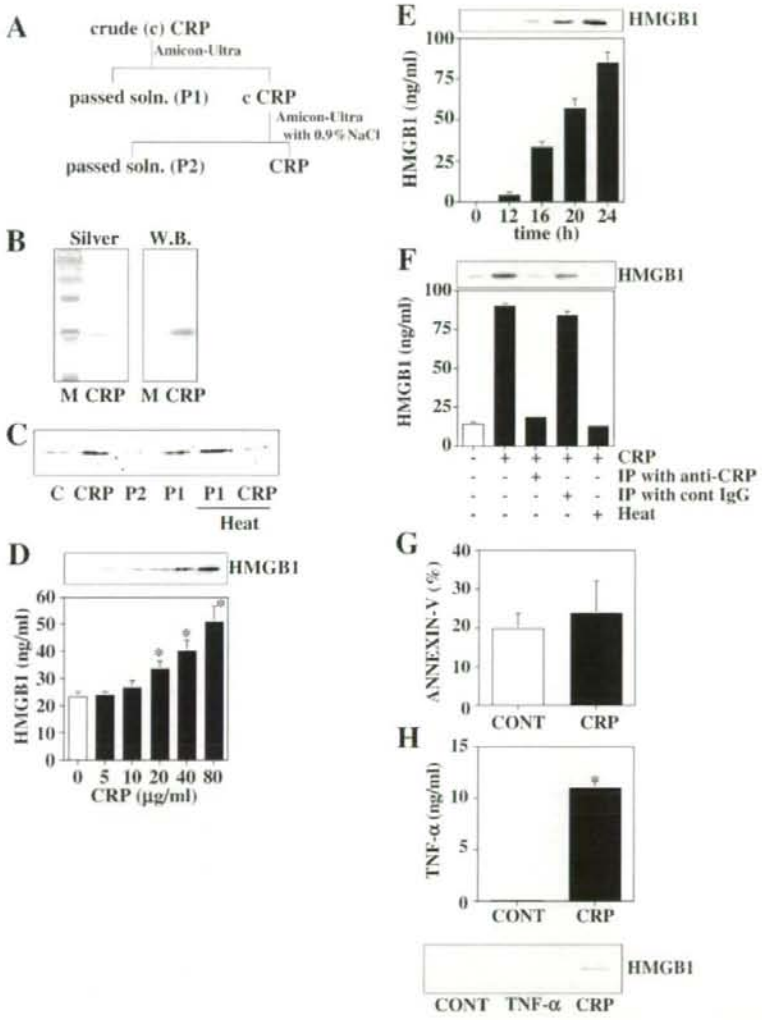

Fig. 1. CRP-induced HMGB1 release by RAW264.7 cells. (A) Schematic presentation of CRP purification with Amicon-Ultra. cCRP was separated with Amicon-Ultra, and the first-pass solution (soln.) was designated as P1. cCRP was washed with LPS-free 0.9% NaCl, and the second-pass solution was designated as P2. (B) Purified CRP was separated with 12% SDS-PAGE. The gels were stained with silver staining (Silver; left) and Western blot analysis (WB; right). (C) The purified CRP induced HMGB1 release. RAW264.7 cells were incubated with pCRP, P1, P2, heated CRP, and heated P1, and the levels of HMGB1 in the supernatants were analyzed for HMGB1 levels by Western blot analysis (upper panel). (D) Dose-dependent effect of CRP. RAW264.7 cells were incubated with CRP (0, 5, 10, 20, 40, and 80 μg/ml) for 20 h. The levels of HMGB1 in the supernatants were analyzed using Western blot analysis (upper panel) and ELISA (lower panel). (E) Time-course effect of CRP. RAW264.7 cells were incubated with CRP (20 μg/ml) for 12, 16, 20, or 24 h. At the end of the treatment, HMGB1 levels were analyzed with Western blot analysis (upper panel) and ELISA (lower panel). (F) RAW264.7 cells were incubated with purified 80 μg/ml CRP (Lane 2); supernatants were obtained by IP with anti-CRP antibody (Lane 3; IP with anti-CRP) or control IgG (Lane 4; IP with control IgG) and heat-inactivated purified CRP (Lane 5) for 24 h; and the levels of HMGB1 in the supernatants were analyzed by Western blot analysis (upper panel) and ELISA (lower panel). (G) Annexin V staining of CRP-treated RAW264.7 cells. RAW264.7 cells were treated with 80 μg/ml CRP for 24 h. Then cells were stained with FITC-labeled Annexin V and analyzed by flow cytometry. (H) Effects of HMGB1 release by TNF-α. RAW264.7 cells were treated with 20 μg/ml CRP for 20 h, and then the TNF-α of supernatants was analyzed by ELISA. RAW264.7 cells were incubated with 50 ng/ml TNF-α or 20 μg/ml CRP for 20 h, and then the HMGB1 of the supernatants was analyzed by Western blot analysis. *Statistically significant ($P<.05$) changes. Note that HMGB1 was released by CRP in RAW264.7 cells, but not TNF-α, under our conditions.

supernatants were analyzed for HMGB1 levels by Western blot analysis.

2.14. Statistical analysis

Statistical analysis was performed using Student's *t* test. Statistical significance was set at $P=.05$.

3. Results

3.1. CRP dose dependently and time dependently triggers the active release of HMGB1 by murine macrophage RAW264.7 cells

Macrophage activation is central to the progression of multiple diseases via the release of inflammatory mediators, including cytokines. CRP has been suggested to directly induce inflammatory responses; therefore, we sought to investigate whether CRP, a biomarker of acute-phase inflammation, triggers the release of HMGB1, a potent late-phase mediator of inflammation by macrophage RAW264.7 cells. However, to rule out the possibility that the effects of CRP were due to biologically active contaminants such as sodium azide and LPS, we first proceeded to purify CRP. The purification steps of CRP are shown schematically in Fig. 1A. As presented in Fig. 1B, crude CRP (cCRP), after filtration with Amicon-Ultra and 12% SDS-PAGE, showed a 25-kDa single band corresponding to CRP after the staining of the gels with sensitive silver staining (left panel) and Western blot analysis (right panel), thus clearly indicating the purity of the CRP.

Purified CRP (20 μg/ml) induced a significant release of HMGB1 by macrophage RAW264.7 cells (Fig. 1C, upper panel, Lane 2) compared to control (Lane 1), although the effect was not observed with heated CRP (Lane 6). On the other hand, Amicon-Ultra passed Solution-1-induced (P1; Lane 4), but not Solution-2-induced (P2; Lane 3), HMGB1 release. These findings suggested that the purified CRP (without either sodium azide or LPS) could induce a significant release of HMGB1 by macrophage RAW264.7 cells. A previous study has demonstrated that extracellular HMGB1 originates from activated monocytes or macrophages and necrotic cells [15]. Next, we examined whether the purified CRP, within a pathophysiological range of concentrations, stimulated macrophage RAW264.7 cells to release HMGB1. For this, we treated macrophage 264.7 cells with various concentrations (5, 10, 20, 40, and 80 μg/ml) of the purified CRP for 20 h. HMGB1 was not detected in the cultured medium in the absence of CRP, whereas at a concentration of as low as 5 μg/ml, CRP triggered a marked increase in HMGB1 levels that was significantly up-regulated at ≥20-μg/ml concentrations of CRP, as determined by Western blot analysis (Fig. 1D, upper panel) and ELISA (Fig. 1D, lower panel). Next, we evaluated the time-course effects of CRP stimulation on HMGB1 release. HMGB1 was detected in the cultured medium after 12 h and continued to increase up to 24 h in response to 20 μg/ml CRP (Fig. 1E). We further confirmed the specific action of CRP on the release of HMGB1 by stimulating cells with heat-inactivated purified CRP or supernatants that were obtained by IP of the purified CRP with anti-CRP antibody or control IgG for 24 h. As shown in Fig. 1F, IP or heat inactivation of the purified CRP caused a marked abrogation of HMGB1 release (control, Lane 1, 13.7±1.7 ng/ml; CRP, Lane 2, 89.7±1.6 ng/ml; CRP+anti-CRP (IP), Lane 3, 13.8±1.7 ng/ml; CRP+control IgG (IP), Lane 4, 84.7±2.2 ng/ml; heat-inactivated CRP, Lane 5, 12.2±0.9 ng/ml), whereas nonimmune control IgG exhibited no loss of CRP activity (Lane 4, 84.7±2.2 ng/ml). Since HMGB1 can be released passively from the nucleus into the cytosol and extracellular space following necrotic cell death, we examined whether the CRP-induced release of HMGB1 originated from necrotic cells. As shown in Fig. 1G, no significant cell death was observed by fluorescence-activated cell sorter (FACS) analysis using Annexin V staining after exposure to CRP (up to 80 μg/ml) for 24 h. To further confirm that the CRP-induced release of HMGB1 by RAW264.7 cells was accompanied by activation of the cells, we evaluated the release of cytokine TNF-α in culture supernatants of CRP-treated RAW264.7 cells by ELISA. As shown in Fig. 1H (upper panel), CRP induced a significant

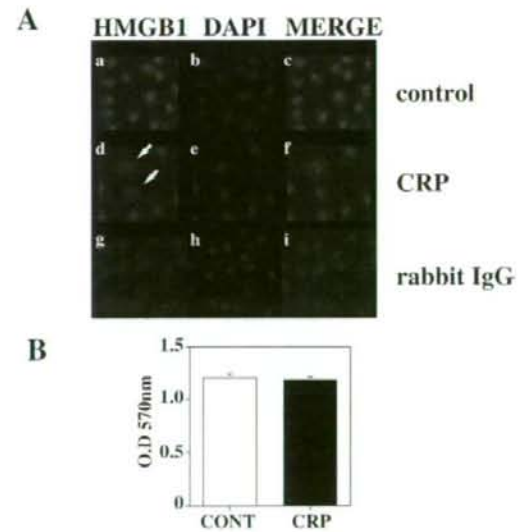

Fig. 2. Nuclear translocation of HMGB1 in response to CRP. (A) RAW264.7 cells were incubated with or without CRP (20 μg/ml) for 16 h. Nontreated (a–c) and CRP-treated (d–f; arrow) cells were incubated with rabbit anti-HMGB1 polyclonal antibody, then with FITC-labeled anti-rabbit IgG as a secondary antibody. As a control IgG, cells were treated with normal rabbit IgG (g–i). Nuclei were labeled with DAPI (original magnification ×400). Arrows indicate nuclear translocation of HMGB1. (B) Effects of CRP on cell viability. Cells were incubated with CRP (20 μg/ml), and the viability of the cells was evaluated by MTT assay. Values are presented as mean±S.D. The data shown are representative of three independent experiments.

release of TNF-α (10±2 ng/ml) compared to control (in the absence of CRP). However, 50 ng/ml TNF-α (fivefold of CRP-induced levels) failed to induce the release of HMGB1 by RAW264.7 cells under the same experimental conditions (Fig. 1H, lower panel). Consistent with this result, anti-TNF-α antibody failed to significantly suppress CRP-induced HMGB1 release (data not shown). These results collectively indicated that CRP stimulated the active release of HMGB1 by RAW264.7 cells and that this was not mediated by cytokine elaboration (at least not through a TNF-α-dependent manner, although we cannot rule out the possible involvement of other cytokines).

3.2. Nuclear translocation of HMGB1 in response to CRP

We next investigated whether CRP stimulation influenced HMGB1 cellular localization. Immunofluorescence analysis revealed that CRP (20 μg/ml) stimulation caused a distinct translocation of nuclear HMGB1 to the cytoplasm (Fig. 2A, d–f, arrow), whereas HMGB1 was observed only in the nucleus in controls (without CRP stimulation) (Fig. 2A, a–c). As expected, no nuclear translocation of HMGB1 was observed in CRP-treated cells that were stained with control

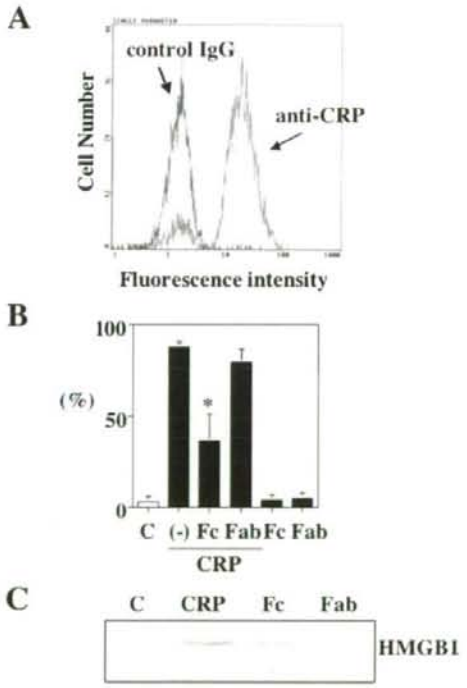

Fig. 3. CRP induced HMGB1 release through the Fcγ receptor. (A) Direct binding of CRP with RAW264.7 cells. The cells were exposed to CRP (20 μg/ml) for 2 h, then incubated with anti-CRP antibody (anti-CRP) or rabbit IgG (control IgG). Next, the cells were incubated with FITC-labeled anti-rabbit IgG antibody and analyzed by flow cytometry. (B) Inhibition of CRP binding by IgG–Fc fragment. Cells were pretreated with Fc fragment (Fc; 1 μM) or Fab fragment (1 μM) for 30 min, then incubated with CRP for 30 min. Cells were then incubated with FITC-labeled anti-CRP rabbit IgG antibody and analyzed by flow cytometry. *Statistically significant ($P<.05$) changes (significantly decreased compared to CRP; Lane 2). (C) HMGB1 release by Fc. CRP was incubated with or without Fc or Fab in RAW264.7 cells, and supernatants were analyzed for HMGB1 levels by Western blot analysis.

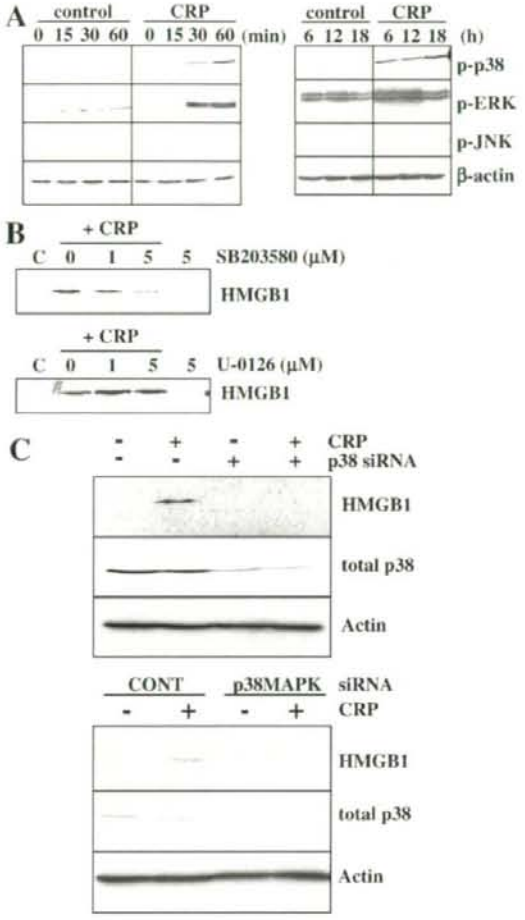

Fig. 4. CRP-induced HMGB1 release mediated by p38MAPK activation. (A) CRP triggered the activation of MAPKs. RAW264.7 cells were incubated with CRP (20 μg/ml) for 0–18 h. Activation of p38MAPK, ERK1/2, and JNK was assayed by Western blot analysis with antibodies specific for p-p38MAPK, pERK1/2, and p-JNK1/2 as, described in Materials and Methods. β-Actin was used as a loading control. Each test represents three separate experiments. (B) RAW264.7 cells were pretreated with SB203580 (1 and 5 μM) or U-0126 (1 and 5 μM) for 15 min, and then incubated with CRP (20 μg/ml) for 20 h. The levels of HMGB1 released into the supernatants were analyzed by Western blot analysis. (C) p38MAPK siRNA inhibited CRP-induced HMGB1 release and p38MAPK expression. RAW264.7 cells were transfected with siRNA for p38MAPK (upper panel) or control (lower panel), and then incubated with CRP (20 μg/ml) for 20 h. The levels of HMGB1 in the supernatants and the expression of p38MAPK were analyzed by Western blot analysis with anti-HMGB1 antibody and anti-total p38MAPK antibody, respectively. Actin was used as a loading control. The data shown are representative of three independent experiments.

IgG instead of HMGB1 (Fig. 2, g–i). Furthermore, as shown Fig. 2B, CRP (20 μg/ml) did not significantly induce cell death as evaluated by MTT assay.

3.3. CRP-induced HMGB1 release is mediated through the Fcγ receptor

Human CRP has been shown to bind directly to murine macrophages through the Fcγ receptor [10,14,25–28], which is also expressed in RAW264.7 cells [29]. We therefore examined whether the CRP-stimulated release of HMGB1 by RAW264.7 cells was mediated by the Fcγ receptor through flow cytometry analysis. CRP was found to bind directly to RAW264.7 cells (Fig. 3A), and this binding was significantly suppressed (about 40% compared to nontreated cells) when cells were pretreated with mouse IgG–Fc fragment (Fc), but not IgG–Fab fragment (Fab) (Fig. 3B). Furthermore, Fc, but not Fab, significantly induced HMGB1 release from cells (Fig. 3C), suggesting that CRP bound directly to the RAW264.7 cells through the Fcγ receptor.

3.4. CRP triggers the activation of ERK1/2 and p38MAPK, but not JNK

Recent studies have demonstrated that CRP activates MAPKs (ERK1/2, JNK, and p38MAPK) through the Fcγ receptor [30,31]. We examined whether CRP stimulation accompanied the activation of MAPKs in RAW264.7 cells by Western blot analysis. CRP stimulation caused a marked activation of MAPKs, p38MAPK, and ERK1/2, but not JNK, in RAW264.7 cells (Fig. 4A, left panel). In parallel, β-actin was used as a loading control in Western blot analysis. p38MAPK and ERK1/2 activation was detected within 30 min, dramatically increased for 1 h, and was thereafter sustained for 18 h (right panel). However, a weak activation of ERK1/2, but not p38MAPK, was observed in nonstimulated cells (control). These results raise the possibility that CRP-induced HMGB1 release may be accompanied by the activation of ERK1/2 and p38MAPK.

3.5. Involvement of p38MAPK in CRP-induced HMGB1 release

We then evaluated the role of the activation of MAPKs p38MAPK and ERK1/2 in HMGB1 release by examining whether specific inhibitors for p38MAPK (SB203580) and ERK1/2 (U-0126) could suppress CRP-induced HMGB1 release by RAW264.7 cells. Cells were treated with SB203580 (1 or 5 μM) or U-0126 (1 or 5 μM) for 60 min prior to CRP stimulation and were then left in the culture until harvest at 20 h poststimulation. It was found that SB203580 (dose dependently), but not U-0126, significantly suppressed CRP-induced HMGB1 release (Fig. 4B). We further confirmed the results by knocking down p38MAPK in RAW264.7 cells using specific siRNA of p38MAPK. RAW264.7 cells transfected with p38MAPK siRNA showed marked suppression of p38MAPK expression and complete inhibition of CRP-induced HMGB1 release (Fig. 4C, upper panel) —effects that were not exhibited by RAW264.7 cells that had been transfected with control siRNA (Fig. 4C, lower panel).

4. Discussion

In this study, we have demonstrated that purified CRP (sodium azide and LPS free) induced an active release of HMGB1 in a time- and dose-dependent manner by macrophage RAW264.7 cells through the Fcγ receptor. This induction of HMGB1 release was completely abrogated by heat inactivation or IP of the purified CRP with anti-CRP antibody, again confirming that this effect of CRP was not caused by LPS contamination. CRP at concentrations of >5 pg/ml has been shown to stimulate cultured human monocytes to release the inflammatory cytokines IL-1β, TNF-α, and IL-1β—an effect that is unaffected by polymyxin B but is cancelled by boiling CRP [32], thus implying that the purified CRP can trigger the release of inflammatory cytokines. Moreover, no loss of cell viability was observed in response to CRP (up to 80 μg/ml) for 24 h, as judged by MTT assay and FACS analysis using Annexin V staining. CRP was also found to stimulate the cells to induce a significant release of TNF-α (an inflammatory cytokine) and to slightly express PGE_2(120±10 pg/ml). On the other hand, CRP did not induce matrix metalloproteinases 2 and 9 in RAW264.7 cells (data not shown). Although CRP induced a significant release of TNF-α, anti-TNF-α antibody failed to significantly suppress CRP-induced HMGB1 release (data not shown). These findings thus further confirm that CRP-induced release of HMGB1 was due to the activation, but not the death, of cells and further indicated that the effect of CRP was not mediated by cytokine elaboration, at least not in a TNF-α-dependent manner, although we cannot rule out the possible involvement of other cytokines.

The concentrations of CRP (5–80 μg/ml) used in the present study are equivalent to those observed in obesity and cardiovascular diseases [33–36]. The finding of the present study—that pathophysiological ranges of CRP induced a significant release of HMGB1 by macrophages—thus highlights an important pathophysiological role for CRP in many inflammatory systems.

The p38MAPK signaling pathway plays an important role in promoting inflammatory diseases [37–39]. Activation of p38MAPK induces the production of key inflammatory mediators, including TNF-α, IL-1β, and HMGB1 [38–40], suggesting that p38MAPK is an obvious therapeutic target for chronic inflammatory diseases. In the current study, we observed that CRP triggered the activation of ERK1/2 and p38MAPK, which was sustained up to 18 h. We examined the functional relationship between MAPK activity and the HMGB1-releasing process. We found that p38MAPK, but not ERK1/2 MAPK, activity played a crucial role in CRP-induced HMGB1 release, as SB203580 (the pharmacological